JOURNAL OF PHYSICAL ORGANIC CHEMISTRY, VOL. 3, 95–109 (1990)

BRØNSTED COEFFICIENTS AND THE THEORY OF ACID–BASE CATALYSIS OF PROTON TRANSFERS FROM CARBON ACIDS

LUÍS G. ARNAUT AND SEBASTIÃO J. FORMOSINHO
Departamento de Química, Universidade de Coimbra, 3049 Coimbra Codex, Portugal

The intersecting-state model previously used to interpret proton transfers in ground and excited states and enzyme catalysis was applied to the general acid–base catalysis of carbon acids. The results are consistent with the predictions published for these systems and provide a new physical meaning for the Brønsted coefficients. It is shown that in addition to the linear free energy effect, the Brønsted coefficients are also influenced by the tightness of the transition states and by electronic effects. The model suggests that the increased reactivity of carbon acids towards proton transfer in non-hydrogen-bonding solvents is caused by an added electronic effect on the thermodynamics of the reactions. The curvatures of the Brønsted plots are interpreted in terms of an entropic contribution to the position of the transition state.

INTRODUCTION

Acid–base catalysis has been extensively studied both theoretically and experimentally. Within this field, the catalysis of reactions of carbon acids by oxygen or nitrogen bases has been the focus of much attention. The systems involved can be represented by the equation

$$RCHXY + B^z \rightleftharpoons RCXY^- + BH^{z+1}$$

where the rate constant for the activated carbon acid deprotonation is k^B and the rate constant for the reverse protonation is k^{BH}. The interest in this type of catalysis comes from both its importance as a tool in synthetic organic chemistry and its theoretical simplicity.

Carbon acid catalysis has attracted so much interest because it is directly relevant to the understanding of some of the most important processes in organic chemistry, which may occur concertedly or in steps, such as the following:

1. The addition of weakly basic nucleophiles to carbonyl compounds:[1,2]

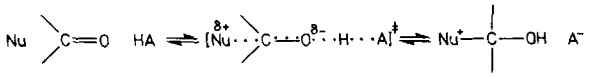

2. Nucleophilic additions to activated olefins:[1,3]

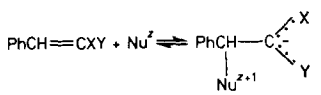

where X and/or Y are activating groups such as CN^-, CO_2^- or NO_2^-;

3. Addition of water or alcohols to electrophilic centres:[1,4]

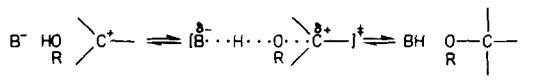

4. Ketonization of enols:[5]

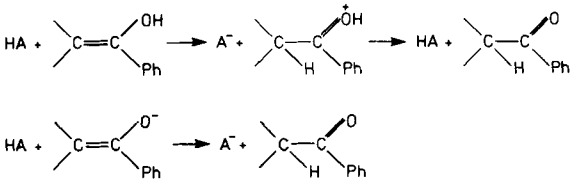

The theoretical simplicity of acid–base catalysis led many workers to use it as a testing ground for reactivity models and linear free energy relationships. These reactions whose rate determining step is a direct proton transfer, are, next to the electron-transfer reactions, the simplest processes that it is possible to find in chemistry. The most popular theoretical framework to rationalize these processes has been the relationship proposed by Brønsted and Pederson over 60 years ago.[6] This relationship establishes the dependence of the catalytic rate constant for acid catalysis, and the equilibrium constant of the catalyst, K_a:

$$k^{HB} = G_a K_a^{\alpha} \qquad (1)$$

where G is a constant dependent only on temperature, pressure, medium and substrate and α, which is independent of the nature of the substrate, has a constant

0894–3230/90/020095–15$07.50

Received 2 January 1989
Revised 20 April 1989

value between 0 and 1 for acids of the same type. A similar equation may be written for the reverse base catalysis, $k^B = G_b K_a^{-\beta}$, and $\alpha + \beta = 1$. It was only 30 years after the formulation of the Brønsted catalysis law that a physical meaning for α (and β) was found: according to Leffler's postulate,[7] the slope of a rate-equilibrium logarithmic relationship measures the position of the transition state along the reaction coordinate. A corollary of this postulate is that the coefficients α and β can be used as reaction progress variables.

Together with the Brønsted relationship, the Marcus rate theory[8] has also been applied to acid–base catalysis. According to Marcus, the free energy of activation, $\Delta G^{\neq}$, and the standard free energy change, ΔG^0, of a proton transfer reaction are related by the expression

$$\Delta G^{\neq} = \Delta G_0^{\neq} (1 + \Delta G^0 / 4\Delta G_0^{\neq})^2 \qquad (2)$$

where $\Delta G_0^{\neq}$ is the 'intrinsic' barrier or value of $\Delta G^{\neq}$ when ΔG^0 is zero; this 'intrinsic' barrier is associated with an 'intrinsic' rate constant, k_0. This theory predicts a curved logarithmic relationship between rate and equilibrium constants. The commonly observed linear relationship, on which Brønsted based his law, is explained on the basis of the experimental use of narrow pK_a ranges.

The existence of a downward curvature in Brønsted plots has been subject to controversy.[9] Such a curvature would be evidence for the validity of the Hammond postulate[10] and Leffler's interpretation of Brønsted plots, because it would reflect a change in transition state structure from product-like in endergonic reactions ($\alpha \rightarrow 1$) to reactant-like in exergonic reactions ($\alpha \rightarrow 0$). Although there is evidence of such curvatures in series of closely related catalysts, as within the family of carboxylate ions,[9] this has been attributed to increased solvation of the anionic bases with increasing basicity. Actually, the fact that the Brønsted plots for primary amines covering a similar pK_a range as the carboxylate ions were linear was taken as evidence against a Hammond–Leffler effect.

Further evidence against this effect comes from the observation that α (or β) does not change with the reaction energy as predicted by the Marcus theory. According to Koeppl and Kresge,[11] the slopes of the nearly linear portions of the Brønsted plots are considerably greater than predicted by Marcus; for example, in base catalysis when the energy of the catalysed reaction is 439 kJ mol^{-1}, the discrepancy between the calculated and experimental slope within the range $\alpha = 0{\cdot}2$–$0{\cdot}8$ may amount to a factor of 2.

Another difficulty with the previously mentioned theories comes from the inequality sometimes observed between the Brønsted β_B values (variation of base) and the Brønsted α_{CH} values (variation of carbon acid). This phenomenon, which is greatest in hydroxylic solvents, is referred to as 'imbalance'. Bernasconi *et al.*[12] attempted to explain the observation of imbalances through the principle of imperfect synchronization: a factor such as hydrogen bonding, resonance, solvation, electrostatic and steric effects, which stabilizes reactants will decrease k_0 if it is lost early and increase k_0 if it is lost late. The terms 'early' and 'late' are defined in relation to the proton transfer step, or the transfer of the negative charge from the base to the carbon acid. Again, in this theory the measurement of the progress of charge transfer in the transition state relies on the experimentally determined values of β_B (or α_{BH}).

All these theoretical studies circle around the physical meaning of the slopes of Brønsted plots first postulated by Leffler. However, this meaning has been seriously questioned theoretically[13] and numerous experimental 'anomalies' have been observed.[14] Therefore, in order to understand and predict the mechanisms and kinetics of acid–base catalysis, it is very important to assess quantitatively, using a molecular viewpoint, the meaning and the limitations of Brønsted coefficients.

The intersecting-state model recently developed to estimate activation energy barriers of chemical reactions[15] has already been used to predict the conditions under which Brønsted coefficients may represent the extent of proton transfer.[16] Now we shall test such predictions systematically and show how this model can be used to rationalize both the curvature of Brønsted plots and its physical meaning. This model can provide valuable information about transition-state structures, namely on the causes of the observed imbalances, solvent effects and synchronism of proton transfers to and from carbon.

INTERSECTING-STATE MODEL

The intersecting-state model (ISM) now used to explain acid–base catalysis has been discussed in detail elsewhere.[15,17] This model has already been applied to proton transfers both in ground[16,18] and excited states.[19] Further, the same theoretical model was also used to interpret a particular type of catalysis, namely enzyme catalysis.[20] Details of the formulation of the model can be found in these and other[21–23] applications of ISM to chemical kinetics. Therefore, here we shall only state the major features of ISM.

We represent the transfer of a proton between a carbon acid and a catalyst in terms of independent bond-breaking and bond-forming processes along a one-dimensional coordinate. This coordinate is given by the sum of the equilibrium bond lengths of reactant and product:

$$d = \eta(l_r + l_p) \qquad (3)$$

where η is a reduced bond distension:

$$\eta = (a' \ln 2/n^{\neq}) + (a'/2)(\Delta G^0/\lambda)^2 \qquad (4)$$

a' is a constant ($a' = 0{\cdot}156$), $n^{\neq}$ is the bond order of

the transition state defined by counting the electrons and λ is an energy associated with the 'mixing or configuration entropy' proposed by Agmon and Levine.[24] The vertical axis associated with bond-breaking and bond-forming processes is assumed to be, as usual, a free-energy coordinate. The changes in this coordinate are determined by the force constants of the bond that is broken, f_r, and that which is formed, f_p, both treated as harmonic oscillators (Figure 1).

From the intersection of the potential (free-energy) curves corresponding to reactants and products, we can calculate $\Delta G^{\neq}$. Now, making use of the Arrhenius-type expression

$$k = (k_B T/h)\exp(-\Delta G^{\neq}/RT) \quad (5)$$

we can obtain the rate constant for a given reaction. For the reverse reaction rate constant the same equation is applied, but the activation free energy becomes $\Delta G^{\neq}_{rev} = \Delta G^{\neq} - \Delta G^0$.

In our calculations we optimize one parameter, d, to reproduce each statistically corrected rate constant for carbon acid deprotonation in base catalysis, k^B, or the reverse rate constant for protonation in acid catalysis, k^{HB}. All the other data necessary for the kinetic calculations (force constants, bond lengths, reaction free energies, temperatures, statistical corrections) can be obtained from tables of thermodynamic and structural experimental determinations. The optimization of d for each reaction corresponds to the empirical determination of $n^{\neq}$ and λ for each reaction. If the application of ISM to acid–base catalysis is physically meaningful, structurally related catalysts and carbon acids will have common values of $n^{\neq}$ and/or λ, otherwise the model will yield scattered results and will be of no practical use.

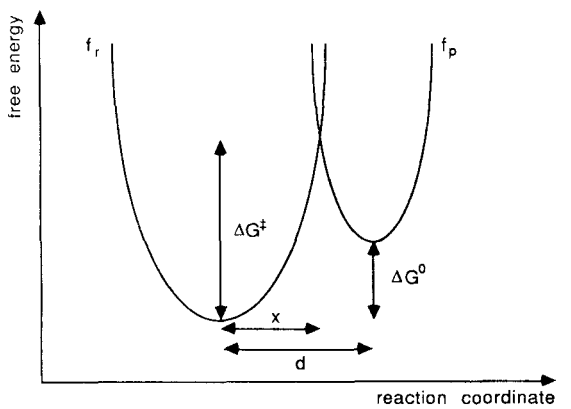

Figure 1. Harmonic potential energy curves representing C—H and H—B bonds in general acid–base catalysis of proton transfers from/to carbon. The force constants for these bonds are f_r and f_p; ΔG^0 = reaction free energy; $\Delta G^{\neq}$ = activation free energy; x = reactant bond distension; d = total bond distension of reactant and product

The previous work with ISM has shown that the Brønsted relationship, as a linear free-energy relationship, will hold just as long as $n^{\neq}$ is constant.[17] Further, meaningful Brønsted coefficients can only be extracted from reaction series with high λ values ($\lambda > 90$ kJ mol^{-1}).[16] The present applications of ISM provide a critical test of these predictions.

THEORETICAL RESULTS AND DISCUSSION

First, we applied ISM to the catalysis of eight carbon acids by series of oxygen and nitrogen bases (Tables 1–4). The results obtained are in agreement with the predictions previously published for these systems:[16] each series of structurally related base catalysts is characterized by a common $n^{\neq}$ and a large λ, i.e. a common intercept and slope for the plots of η versus $(\Delta G^0)^2$ (Figures 2 and 3). These series lead to the well known straight lines in ln k vs pK_a plots, which define the 'Brønsted families.' The only relevant exception, in terms of both ISM and Brønsted plots, is the catalysis by 2,6-dimethylpyridine, which shows significantly larger η values than the catalysis by other pyridines; this increase in η can be assigned to steric effects. The results for H_2O and OH^- are also peculiar. Some workers have interpreted the catalysis by OH^- together with that by carboxylate ions and the catalysis by H_2O together with amines.[25] Our model does not support such a grouping of the catalysts, because they do not seem to have common n *and* λ values. In the present calculations, we used the acidity constants of water and hydroxide ions considering the concentration of water on the molar scale.[14] This method of calculation leads to acidity constants consistent with those for the other catalysts and does not account for the possibility of proton transfer through the Grotthuss chain mechanism, as we have considered previously,[16,19] because carbon acids do not form hydrogen bonds to water. We shall postpone further discussion on this subject until we study solvent effects.

A deeper analysis of the data in Tables 1–4 can be made according to two guidelines: the discussion of the differences among each series of catalysts for a given carbon acid and of the differences among the several carbon acids for the same catalyst.

Substitution in the oxygen/nitrogen catalyst

The comparison between the several types of catalysts allows us to establish the following hierarchy of $n^{\neq}$ values: $n^{\neq}_{RNH_2} < n^{\neq}_{R_2NH} \approx n^{\neq}_{RCOO^-} < n^{\neq}_{\phi O} \approx n^{\neq}_{R_2N}$ (Table 5). The magnitude of the $n^{\neq}$ values for the secondary, primary and aromatic amines seems to be related to their degree of solvation, because the degree of hydrogen bonding with the solvent seems to depend on the number of hydrogen atoms in the cation.[26] This

Table 1. Bond distensions for base catalysis of carbon acids, $R_3CH + B \rightarrow R_3C + HB$, in Me_2SO–water(1 : 1), at 293 K[a]

Catalyst and pK_a^{BH}	Acetylacetone[b] ($pK_a^{CH} = 9{\cdot}12$) k^B/l mol^{-1} s^{-1}	ΔG^0 and $\Delta G^{\neq}$/kJ mol^{-1}	d/pm and 100η	1,3-Indandione[c] ($pK_a^{CH} = 6{\cdot}35$) k^B/l mol^{-1} s^{-1}	ΔG^0 and $\Delta G^{\neq}$/kJ mol^{-1}	d/pm and 100η	Benzylidene-1,3-indandione[d] ($pK_a^{CH} = 5{\cdot}87$) k^B/l mol^{-1} s^{-1}	ΔG^0 and $\Delta G^{\neq}$ kJ mol^{-1}	d/pm and 100η
$RCOO^-$:									
Cl_2CH	$4{\cdot}0 \times 10^{-2}$	42·5	36·7				1·6	22·6	37·2
2·15		79·5	181					70·6	183
$NCCH_2$	$2{\cdot}2 \times 10^{-1}$	36·1	36·5	$1{\cdot}3 \times 10^{1}$	20·5	35·9			
3·29		75·4	180		65·5	177			
$ClCH_2$	$4{\cdot}3 \times 10^{-1}$	33·7	36·4	$2{\cdot}5 \times 10^{1}$	18·2	35·7	$1{\cdot}4 \times 10^{1}$	13·8	36·9
3·71		73·9	179		63·8	176		65·5	182
$MeOCH_2$	1·3	29·0	36·3	$35{\cdot}9 \times 10^{1}$	13·4	35·8			
4·56		71·1	179		61·9	177			
$ClCH_2CH_2$	2·9	25·4	36·3						
5·20		69·2	179						
CH_3	5·2	22·1	36·3	$2{\cdot}4 \times 10^{2}$	6·6	35·8	$1{\cdot}5 \times 10^{2}$	2·2	36·8
5·78		67·6	179		58·5	177		59·4	181
RNH_2:									
$NCCH_2$	2·1	19·9	38·2	$8{\cdot}4 \times 10^{1}$	4·4	37·7			
5·39		70·0	183		60·8	181			
$EtOOCCH_2$	$2{\cdot}8 \times 10^{1}$	6·2	38·3	$1{\cdot}3 \times 10^{3}$	−9·3	37·6			
7·83		63·5	184		54·2	181			
H_2NCOCH_2	$3{\cdot}5 \times 10^{1}$	3·7	38·5	$1{\cdot}1 \times 10^{3}$	−11·8	38·2			
8·28		63·0	185		54·9	183			
$MeO(CH_2)_2$	$1{\cdot}5 \times 10^{2}$	−3·8	38·5	$4{\cdot}9 \times 10^{3}$	−19·4	38·0			
9·63		59·5	185		51·1	183			
n-Bu	$4{\cdot}9 \times 10^{2}$	−9·7	38·4	$1{\cdot}7 \times 10^{4}$	−25·3	37·8			
10·68		56·5	184		47·9	181			
Morpholine	$2{\cdot}5 \times 10^{2}$	2·4	37·2	$9{\cdot}0 \times 10^{3}$	−13·2	36·6			
8·70		58·3	179		49·4	176			
Piperidine	$2{\cdot}4 \times 10^{3}$	−10·8	37·4	$7{\cdot}9 \times 10^{4}$	−26·4	36·7	$3{\cdot}9 \times 10^{4}$	−30·8	37·9
11·05		52·7	179		44·1	176		46·0	182
PhO^-:									
4-CN				$2{\cdot}6 \times 10^{4}$	−11·4	34·7			
8·69					47·0	171			
3,5-Cl_2				$5{\cdot}9 \times 10^{4}$	−12·4	34·1			
8·87					44·8	168			
3-Cl				$1{\cdot}2 \times 10^{5}$	−19·5	34·5			
10·12					43·1	170			
4-Cl				$1{\cdot}4 \times 10^{5}$	−21·7	34·8			
10·51					43·0	171			
H				$2{\cdot}1 \times 10^{5}$	−26·6	35·1	$4{\cdot}6 \times 10^{4}$	−31·0	36·8
11·40					42·0	173		45·5	181
3,5-Me_2				$3{\cdot}7 \times 10^{5}$	−28·1	34·8			
11·66					40·5	172			
H_2O	$2{\cdot}1 \times 10^{-4}$	58·3	37·9	$1{\cdot}1 \times 10^{-2}$	34·6	39·0	$1{\cdot}8 \times 10^{-2}$	38·3	38·1
−1·44		92·2	187		82·7	192		81·5	188
OH^-	$3{\cdot}1 \times 10^{4}$	−46·1	38·9	$3{\cdot}4 \times 10^{5}$	−53·6	40·4	$2{\cdot}8 \times 10^{5}$	−66·0	39·4
17·34		46·6	192		48·7	199		41·0	194

[a] $f_r = 290$ J mol^{-1} pm^{-2}; $f_p = 420$ J mol^{-1} pm^{-2} ($f_p = 380$ J mol^{-1} pm^{-2} for amines); $l_r + l_p = 202{\cdot}8$ pm ($l_r + l_p = 208{\cdot}3$ pm for amines).[36]
[b] Ref. 9.
[c] Ref. 25.
[d] Ref. 37.

Table 2. Bond distensions for base catalysis of carbon acids, $R_3CH + B \rightarrow R_3C + HB$, in Me_2SO–water(1 : 1), at 298 K[a]

Catalyst and pK_a^{BH}	2,2′,4,4′-Tetranitrodiphenylmethane ($pK_a^{CH} = 10{\cdot}90$)			2,4,4′-trinitrodiphenylmethane ($pK_a^{CH} = 12{\cdot}19$)		
	k^B/l mol^{-1} s^{-1}	ΔG^0 and $\Delta G^{\neq}$/kJ mol^{-1}	d/pm and 100η	k^B/l mol^{-1} s^{-1}	ΔG^0 and $\Delta G^{\neq}$/kJ mol^{-1}	d/pm and 100η
$RCOO^-$:						
$ClCH_2$	$4{\cdot}2 \times 10^{-5}$	44·5	42·0	$2{\cdot}0 \times 10^{-6}$	51·8	43·0
3·71		98·0	207		105·5	212
H	$1{\cdot}0 \times 10^{-4}$	40·2	42·0	$5{\cdot}5 \times 10^{-6}$	47·6	42·9
4·45		95·8	207		103·0	212
$MeOCH_2$	$1{\cdot}3 \times 10^{-4}$	39·1	42·0	$5{\cdot}7 \times 10^{-6}$	46·5	43·0
4·65		95·3	207		102·8	212
CH_3	$4{\cdot}4 \times 10^{-4}$	32·7	42·0	$2{\cdot}3 \times 10^{-5}$	40·0	43·0
5·78		92·0	207		99·4	212
2-Cl-C_6H_4	$2{\cdot}2 \times 10^{-4}$	41·7	41·2	$1{\cdot}0 \times 10^{-5}$	49·0	42·2
4·20		93·8	203		101·3	208
C_6H_5	$4{\cdot}7 \times 10^{-4}$	36·4	41·5	$2{\cdot}1 \times 10^{-5}$	43·7	42·5
5·13		92·0	204		99·5	210
RNH_2:						
$MeO(CH_2)_2$	$2{\cdot}3 \times 10^{-2}$	9·2	43·5	$1{\cdot}8 \times 10^{-3}$	16·6	44·2
9·11		82·4	209		88·6	212
n-Bu	$8{\cdot}3 \times 10^{-2}$	4·2	43·2	$5{\cdot}5 \times 10^{-3}$	11·5	44·1
9·99		79·1	207		85·8	212
C_6H_5	$1{\cdot}2 \times 10^{-4}$	39·9	42·7	$8{\cdot}5 \times 10^{-6}$	47·3	43·5
3·73		95·3	205		102·0	209
Morpholine	$3{\cdot}5 \times 10^{-2}$	15·2	42·3	$2{\cdot}7 \times 10^{-3}$	22·6	43·1
8·23		81·2	203		87·6	207
Piperidine	$3{\cdot}6 \times 10^{-1}$	3·0	42·4	$2{\cdot}7 \times 10^{-2}$	10·3	43·2
10·38		75·6	203		81·9	207
R-pyridine:						
H	$6{\cdot}6 \times 10^{-6}$	41·7	42·9	$4{\cdot}8 \times 10^{-6}$	49·1	43·6
3·89		96·8	206		103·4	209
4-CH_3	$2{\cdot}7 \times 10^{-4}$	36·8	42·6	$2{\cdot}0 \times 10^{-5}$	44·2	43·3
4·75		93·3	205		99·6	208
3,5-$(CH_3)_2$	$4{\cdot}7 \times 10^{-4}$	35·3	42·5	$3{\cdot}9 \times 10^{-5}$	42·7	43·1
5·01		92·0	204		98·1	207
2,6-$(CH_3)_2$	$7{\cdot}9 \times 10^{-5}$	33·1	44·0	$1{\cdot}1 \times 10^{-5}$	40·5	44·3
5·40		96·3	211		101·2	213
PhO^-:						
2-CN	$1{\cdot}1 \times 10^{-1}$	18·4	40·2	$6{\cdot}0 \times 10^{-3}$	25·8	41·2
7·97		78·6	198		85·6	203
4-CN	$8{\cdot}7 \times 10^{-2}$	15·7	40·7	$6{\cdot}0 \times 10^{-3}$	23·1	41·6
8·45		79·0	201		85·7	205
2-Br	$6{\cdot}2 \times 10^{-1}$	9·6	40·2	$3{\cdot}4 \times 10^{-2}$	17·0	41·2
9·52		74·2	198		81·3	203
4-Cl	1·1	5·8	40·3	$5{\cdot}1 \times 10^{-2}$	13·2	41·4
10·18		72·8	199		80·3	204
H	3·0	−0·1	40·3	$1{\cdot}7 \times 10^{-1}$	7·3	41·4
11·21		70·1	199		77·4	204
4-CH_3O	5·5	−1·5	40·1	$2{\cdot}5 \times 10^{-1}$	5·8	41·3
11·47		68·8	198		76·3	204
H_2O	$4{\cdot}0 \times 10^{-9}$	69·4	44·5	$2{\cdot}7 \times 10^{-10}$	76·8	45·2
−1·44		121·0	220		127·5	223
OH^-	$2{\cdot}3 \times 10^{-1}$	−36·7	43·2	1·1	−29·4	44·5
17·34		65·2	213		72·9	219

[a]For force constants and bond lengths, see Table 1. Thermodynamic and kinetic data from ref. 38.

Table 3. Bond distensions for base catalysis of carbon acids, $R_3CH + B \rightarrow R_3C + HB$, in Me_2SO–water(1 : 1), at 293 K[a]

Catalyst and pK_a^{BH}	(2,4-Dinitrophenyl)acetonitrile ($pK_a^{CH} = 8{\cdot}06$) k^B/l mol^{-1} s^{-1}	ΔG^0 and $\Delta G^{\neq}$/kJ mol^{-1}	d/pm and 100η	(4-Nitrophenyl)acetonitrile ($pK_a^{CH} = 12{\cdot}62$) k^B/l mol^{-1} s^{-1}	ΔG^0 and $\Delta G^{\neq}$/kJ mol^{-1}	d/pm and 100η
$RCOO^-$:						
$ClCH_2$	$3{\cdot}8 \times 10^{-1}$	27·8	37·5			
3·71		74·2	185			
H	$9{\cdot}8 \times 10^{-1}$	23·6	37·4			
4·46		71·8	184			
CH_3	6·0	16·2	37·2			
5·78		67·5	183			
RNH_2:						
$MeO(CH_2)_2$	$5{\cdot}7 \times 10^{2}$	−9·8	38·3	9·4	15·8	37·7
9·63		56·1	184		66·2	181
n-Bu	$2{\cdot}6 \times 10^{3}$	−15·7	38·0	$4{\cdot}8 \times 10^{1}$	9·9	37·3
10·68		52·6	182		62·2	179
Morpholine	$8{\cdot}5 \times 10^{2}$	−3·6	37·1	6·1	22·0	37·0
8·70		55·2	178		67·3	178
Piperidine	$1{\cdot}2 \times 10^{4}$	−16·8	36·9	$3{\cdot}1 \times 10^{2}$	8·8	36·0
11·05		48·7	177		57·7	173
$Me_2AsO_2^-$	$2{\cdot}0 \times 10^{2}$	6·5	35·9			
7·50		58·9	177			
H_2O	$6{\cdot}8 \times 10^{-5}$	52·3	39·9			
−1·44		95·1	197			
OH^-	$1{\cdot}8 \times 10^{5}$	−52·1	38·2	$1{\cdot}3 \times 10^{4}$	−26·5	37·2
17·34		42·1	188		48·7	184

[a]For force constants and bond lengths, see Table 1. Thermodynamic and kinetic data from ref. 30.

Table 4. Bond distensions for base catalysis of $PhCH_2CH(COMe)CO_2Et$ ($pK_a^{CH} = 11.81$) in aqueous solutions at 298 K[a]

Catalyst and pK_a^{BH}	k^B/l mol^{-1} s^{-1}	ΔG^0 and $\Delta G^{\neq}$/kJ mol^{-1}	d/pm	x/pm
$RCOO^-$:				
$ClCH_2$	$1{\cdot}1 \times 10^{-3}$	52·8	38·2	24·9
2·86		89·9		
CH_3CHCl	$1{\cdot}2 \times 10^{-3}$	52·2	38·3	24·9
2·96		89·8		
$ClCH_2CH_2$	$3{\cdot}5 \times 10^{-3}$	46·3	38·4	24·5
4·00		86·9		
C_6H_5	$4{\cdot}3 \times 10^{-3}$	45·1	38·5	24·4
4·21		86·5		
CH_3	$7{\cdot}2 \times 10^{-3}$	42·0	38·6	24·2
4·75		85·3		
CH_3CH_2	$7{\cdot}9 \times 10^{-3}$	41·3	38·7	24·2
4·87		85·1		
test	$2{\cdot}1 \times 10^{-2}$	36·2	38·7	23·9
5·75		82·6		

[a]For force constants and bond lengths, see Table 1. Thermodynamic and kinetic data from ref. 39.

decrease in solvation leads to an increase in the availability of the non-bonding electron pairs to participate in the reaction coordinate and, consequently, in $n^{\neq}$.[23] The $n^{\neq}$ values for all the reactions in Tables 1–4 range from 0·504 to 0.64 (Table 5). This means that the transition state bond order is strongly dominated by the carbon acid bond order, because previous applications of ISM to proton transfer reactions have shown that for oxygen and nitrogen acids $n^{\neq} \approx 0{\cdot}84$ whereas for carbon acids $n^{\neq} \approx 0{\cdot}55$. Consequently, we may say that in general acid–base catalysis, the catalysts will only slightly perturb the electronic distribution of the transition state. Their most significant effect will be an energetic stabilization of the transition state. These are precisely the reasons that lead to the apparent success of Brønsted correlations, i.e. changes in reactivity are dominated by changes in reaction energy.[27] If structural substitutions along a catalyst series were to change $n^{\neq}$, the corresponding changes in k would be difficult to rationalize solely in terms of Brønsted correlations.

Substitution in the carbon acid

Given the fact that $n^{\neq}$ is dominated by the nature of the

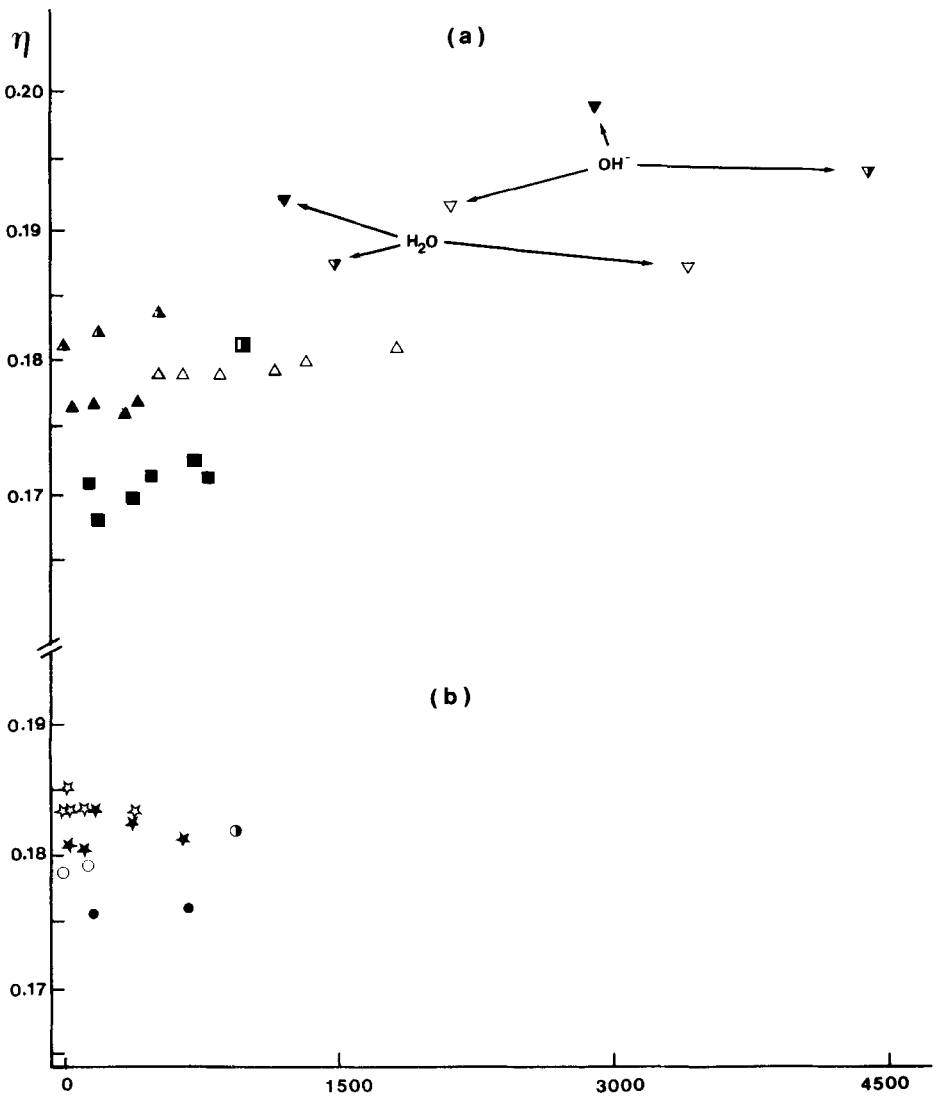

Figure 2. Reduced bond distension, η, as a function of $(\Delta G^0)^2$, for proton transfers from acetylacetone (open points), 1,3-indandione (filled points) or benzylidene-1,3-indandione (half-filled points), to (a) oxygen bases or (b) nitrogen bases. □, $R\phi O^-$; △, $RCOO^-$; ○, R_2NH; ☆, RNH_2. Calculated data in Table 1

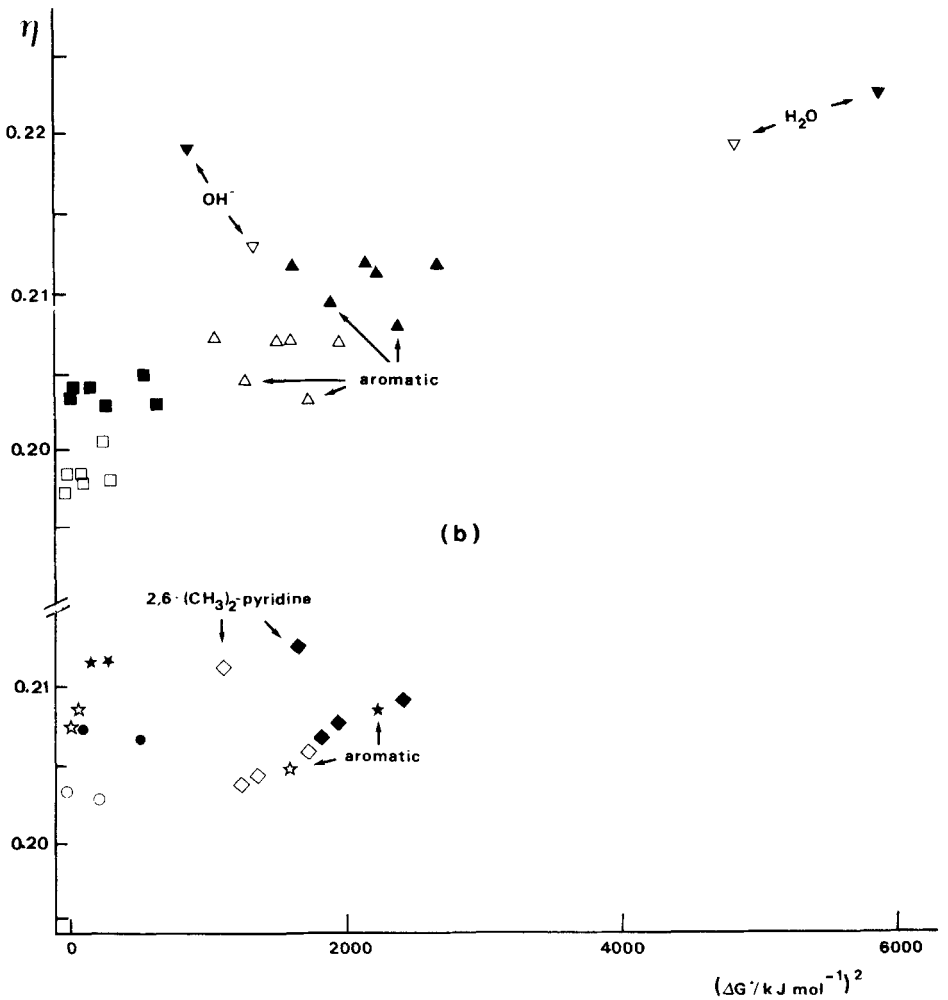

Figure 3. η as a function of $(\Delta G^0)^2$ for proton transfers from 2,2',4,4'-tetranitrodiphenylmethane (open points) or 2,4,4'-trinitrodiphenylmethane (filled points) to (a) oxygen bases or (b) nitrogen bases. □, $R\phi O^-$; △, $RCOO^-$; ◇, R_2N; ○, R_2NH; ☆, RNH_2. Calculated data in Table 2

carbon acid, a number of important consequences can be expected. The most striking one is that a substitution in the carbon acid may lead to a more significant change in $n^{\neq}$ than in the linear dependence on $(\Delta G)^2$, because λ is high and the pK_a range involved is narrow.

A clear analysis of the electronic effects associated with substitution in the carbon acid can be made using a larger series of substituted carbon acids for a common base. The results of this type of calculations are presented in Table 6. The $n^{\neq}$ range involved in these reactions is limited and therefore it is difficult to establish the exact type of dependence between $n^{\neq}$ and a parameter that may translate the variation of the electronic configuration of the transition state. According to the configuration mixing model,[28] fast proton transfers involving oxygen or nitrogen acids can be rationalized with only two configurations, $\{B_1{:}^- H{-}B_2\}$ and $\{B_1{-}H : B_2^-\}$, one for the products and another for the reagents. However, for the carbon acids a third configuration, $\{B_1{:}^- H^+ : B_2^-\}$, is needed because the predominant product configuration is a doubly excited one owing to the required electronic reorganization. We can expect the extra configuration present in carbon acids to exert a specific influence on the transition state bond order, not observed for fast acid catalysis. It is important to keep in mind that the reference configurations for slow and fast proton transfers are different, because each must include specific non-bonded interactions.

The simplest effect that an extra configuration may

Table 5. Transition state bond orders for base catalysis reactions[a]

Carbon acid	$RCOO^-$	RNH_2	R_2NH	$R\phi O^-$
Acetylacetone	0·60	0·586	0·60	
1,3-Indandione	0·61	0·593	0·614	0·64
				(~120)
Benzylidene-1,3-indandione	0·596			
	(140)			
2,2',4,4'Tetranitrodiphenylmethane	0·52	~0·52	0·53	0·545
2,4,4'-Trinitrodiphenylmethane	0·51	0·51	0·52	0·53
2,4-Dinitrophenylacetonitrile	0·593		0·61	
	(165)			
4-Nitrophenylacetonitrile	0·61		0·63	
$PhCH_2CH(COMe)CO_2Et$	0·55			

[a]The values of λ are in general >200 kJ mol^{-1}; for some reactions the experimental data of η versus $(\Delta G^0)^2$ (at least 3 points) allows the estimation of λ values, shown in parentheses (λ/kJ mol^{-1}).

Table 6. Bond distentions and electron affinities for base catalysis of carbon acids by acetate ion ($pK_a^{BH} = 8·06$) in aqueous solution at 298 K[a])

	$RC_6H_4CH_2CH(COCH_3)CO_2CH_2CH_3$				$RC_6H_4CH_2CH(COCH_3)_2$		
Substituent and ΔE_A/eV	k^B/l mol^{-1} s^{-1} and pK_a^{CH}	ΔG^0 and $\Delta G^{\neq}$/kJ mol^{-1}	d/pm and 100 η	x/pm	k^B/l mol^{-1} s^{-1}	ΔG^0 and $\Delta G^{\neq}$/kJ mol^{-1}	d/pm and 100 η
4-CH_3O	$5·9 \times 10^{-3}$	42·4	38·7	24·3	$1·5 \times 10^{-2}$	34·9	39·2
−0·10	11·89	85·8	191		10·57	83·5	193
4-CH_3	$6·2 \times 10^{-3}$	42·3	38·6	24·3			
−0·06	11·88	85·4	190				
3-CH_3	$7·0 \times 10^{-3}$	42·3	38·6	24·3			
−0·02	11·87	85·4	190				
H	$7·2 \times 10^{-3}$	41·9	38·6	24·2	$1·8 \times 10^{-2}$	34·4	39·1
0	11·81	85·2	190		10·49	82·9	193
4-Cl	$9·9 \times 10^{-3}$	40·6	38·6	24·1	$2·0 \times 10^{-2}$	33·0	39·2
0·25	11·57	84·5	190		10·25	82·5	193
4-CN	$1·9 \times 10^{-2}$	38·6	38·4	23·9	$4·3 \times 10^{-2}$	29·8	39·2
0·71	11·23	82·8	189		9·69	80·9	193
4-NO_2	$2·5 \times 10^{-2}$	37·7	38·3	23·8	$5·0 \times 10^{-2}$	29·0	39·2
0·99	11·06	82·0	189		9·54	80·4	193
Test	$3·8 \times 10^{-2}$	36·2	38·3	23·7			
0·99	10·81	81·1	189				

[a]For force constants and bond lengths, see Table 1. Thermodynamic and kinetic data from ref. [39]. Electron affinities of substituents relative to nitrobenzene. [40].

cause is to change the height of the barrier for the reactant encounter complex. This barrier is a fraction of the energy gap between the intersecting configurations:[29]

$$\Delta G^{\neq} = f(I_P - E_A) - B \qquad (6)$$

where I_P is the ionization potential of the electron donor (oxygen or nitrogen base), E_A is the electronic affinity of the substrates (series of substituted carbon acids) and B the splitting due to the avoided crossing. Assuming a small dependence on $(\Delta G)^2$, for the catalysis of a series of carbon acids by a common base, the activation barrier will only depend on E_A. This reveals the existence of an electronic effect that may change $n^{\neq}$ when the carbon acid is changed. This electronic effect is a charge-transfer interaction, which increases with the electronic affinity of the substrate. Such an interaction must increase the transition state bond order, because it increases the electronic density of the reactive configurations at the transition state. Therefore, we can look for an empirical correlation between $n^{\neq}$ and E_A.

Two plots of $n^{\neq}$ as a function of E_A are shown in Figure 4 for the catalysis of the reactions of $XC_6H_4CH_2CH(COMe)CO_2Et$ and $XC_6H_4CH_2CH(COMe)_2$ with acetate ion. We cannot draw firm conclusions from Figure 4, because the range of values involved is limited. However, the change is in

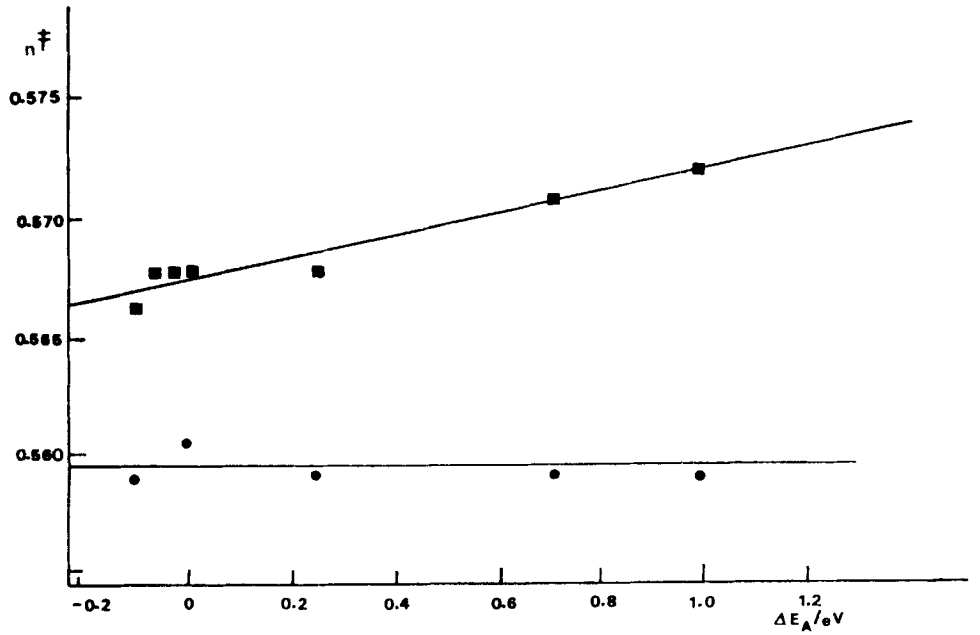

Figure 4. Transition-state bond orders, $n^{\neq}$, as a function of electron affinities, E_A, for proton transfers from $RC_6H_4CH_2CH(COCH_3)CO_2CH_2CH_3$ (squares) or $RC_6H_4CH_2CH(COCH_3)_2$ (circles) to acetate ion. Data in Table 5

the direction predicted by the model and may be relevant for the study of other carbon acids where substitution leads to larger changes in acidity.

The same interpretation can be used to analyse some of the differences among the several carbon acids for the same oxygen or nitrogen base in Tables 1–3. For example, if we compare acetylacetone (AA) with 1,3-indandione (ID), we see that ID has a slightly higher $n^{\neq}$ (Table 5). This can be easily understood by taking into consideration that the benzene ring in ID leads this molecule to a higher E_A compared with the effects of the methyl groups of AA. A direct comparison between these two carbon acids and benzylidene-1,3-indandione (BID) is not possible because in the latter there are opposing electronic and steric effects. The same type of analysis can be extended to 2,2′,4,4′-tetranitrodiphenylmethane (TTND) and 2,4,4′-trinitrodiphenylmethane (TND): the former has a larger $n^{\neq}$ and can be expected to have a higher E_A. The same reasoning can be used to compare TTND and TND with (2,4-dinitrophenyl)acetonitrile (DNA) and (4-nitrophenyl)acetonitrile (NA). The differences between these two pairs of carbon acids can be understood considering that a phenyl group is replaced by a cyano group, which has a higher E_A and must lead to the observed increase in $n^{\neq}$. A similar comparison between NA and DNA cannot be made, because the decrease in η expected from the increased E_A of DNA may be offset by the energetic factor due to the large ΔpK_a between these carbon acids ($\Delta pK_a > 4{\cdot}5$), or by the greater need for solvent reorganization of DNA.[30]

Transition state imbalances

The Brønsted relationship probes the transition state by changing it. Theories based on the meaning of the Brønsted coefficient assume that these changes are small. Actually, the application of ISM to carbon acid catalysis indeed shows that in general the dependence of η on $n^{\neq}$ and $(\Delta G)^2$ is small. Although this explains the apparent linearity of the Brønsted relationship when applied to carbon acids we cannot infer that Brønsted coefficients are a good guide to transition state structure or can even be used as a reaction progress variable. This difficulty with the Brønsted coefficients is evident in the experimental observation of transition state 'imbalances.' For example, the catalysis of $C_6H_5CH_2CH(COMe)CO_2Et$ by a series of carboxylate ions (Table 4) yields $\beta_B = 0{\cdot}44$, whereas the catalysis of $XC_6H_4CH_2CH(COMe)CO_2Et$ by acetate ion (Table 6) leads to $\alpha_{CH} = 0{\cdot}76$. As it is the same transition state that is being probed, we should have $\beta_B = \alpha_{CH}$. According to ISM we can define a normalized progress variable as x/d, where x is the bond extension of the reactant. For the above reactions the numerical result is $x/d = 0{\cdot}62$. The reasons for the disagreement among these values have to be sought in their real physical meaning.

We have already shown that the meaning of changing the carboxylate ions as catalysts is to change the energetic stabilization of the transition state. Two effects operate in this thermodynamic change: the linear free energy and the mixing entropy. The linear free energy effect is translated by the Brønsted coefficient: as the $pK_a^{CO_2H}$ of the carboxylic acid increases, ΔG^0 for the reaction is decreased and, assuming that η remains constant, k^B will increase and β_B tend to zero. If the $pK_a^{CO_2H}$ of the carboxylic acid decreases, then β_B tends to unity. However, as λ is not infinity, η will increase with $(\Delta G^0)^2$, which means that for exothermic reactions this increase leads to less reactant-like transition states and for endothermic reactions it leads to less product-like transition states. The overall result of these contradictory effects will be a reduced sensitivity of β_B to the position of the transition state and the observation of conservative values within the 'normal' limits of zero and unity.

Changing the carbon acid adds an electronic effect to the conventional linear free energy effect. This new factor operates systematically in the same direction: $n^{\neq}$ increases with E_A. In order to understand the influence of $n^{\neq}$ on α_{CH}, we must remember that α is often considered to be equal to the bond order of the bond being formed.[8] Although this equality has been questioned,[13] it is clear that α_{CH} and the transition state bond order are related.[31] Therefore, we can expect α_{CH} to reflect both the conventional linear free energy effect and the changes in $n^{\neq}$. For carbon acids with a large E_A, the bond order at the transition state increases and we can expect the bond order of the bond being broken also to increase. Consequently, α_{CH} will show enhanced values for compounds with high E_A. This electronic effect may explain the exalted α_{CH} values observed for the nitroalkanes.

Another way to rationalize the physical meaning of these probes of the transition state position can be based on the two-dimensional diagrams proposed by More O'Ferrall.[32] In the application of these diagrams to proton transfers involving carbon acids, the two coordinates considered are the degree of proton transfer and the degree of charge delocalization and solvation.[12b] Bernasconi[12b] proposed β_B as the progress coordinate along the first coordinate and defined a new progress variable, α_C^{res}, for the second coordinate. This new progress variable is defined by the ratio between the extent of increase in k^B and the extent of increase in the acidity of the carbon acid caused by a stronger π-acceptor substituent, e.g. by changing from CN to NO_2.

Although these two interpretations of β_B and α_{CH} (or α_C^{res}) may not be entirely compatible, they emphazise the concept that the reaction coordinate has two contributions, one of them related to β_B and the other to a measure of the electronic density in the carbon acid. The reaction coordinate defined by ISM encompasses these two contributions and overcomes the difficulties and inconsistencies of using two progress variables separately. Actually, the arbitrary splitting of the reaction path in two leads to anomalous values for each component.

In order to evaluate the added effects of $n^{\neq}$ and λ on the reaction free energy effect in the position of the transition state of a given reaction, we calculated the influence of changing the pK of the carbon acid or the oxygen base by one unit in the direction of decreasing the endothermicity of the reactions shown in Tables 4 and 6. We extrapolated the rates of proton transfer from the corresponding Brønsted plots, and adjusted the d values for these hypothetical reactions in order to reproduce their estimated rate constants. Our results show that when we decrease the pK_a of the carbon acids by one unit and keep acetate ion as the catalyst, the critical configuration moves in the direction of the reactants by 0·5 pm; however, the change to a carboxylic acid one pK_a unit less acidic for $CH_6H_5CH_2CH^-(COMe)CO_2Et$ as the carbon base the critical configuration moves in this same direction by just 0·3 pm.

According to the current interpretations of the Brønsted relationship, both the change in the carbon acid and the change in the oxygen catalyst should affect the transition state in the same way and lead to identical values of α_{CH} and β_B, because they are equivalent energetic changes, which is in disagreement with the experimental observations. However, ISM does predict the observed behaviour, because the transition state localization is sensitive to changes in the bond orders, to the tightness of the potential and to the asymmetry of the force constants. This is a general result and explains the 'transition state imbalances' commonly observed in carbon acid catalysis by oxygen and nitrogen bases.[12] This interpretation offers a simple alternative to the principle of imperfect synchronization, which is based on solvent effects and the Leffler–Hammond interpretation of α_{CH} and β_B.

Solvent effects

The studies of solvent effects on Brønsted correlations by Bernasconi and co-workers[9,23,33] have shown that an increase in the Me_2SO content in aqueous solutions leads to a curvature of the Brønsted plot of carbon acid catalysis by carboxylic ions. In terms of the ISM, we must be able to assign these observations to a decrease in λ (Table 7). Bernasconi and co-workers also showed that the presence of Me_2SO leads to a large increase in k^B, part of it caused by the more favourable thermodynamics of the reaction and part by the decrease in the intrinsic barrier. According to the ISM, the changes in the energy barrier of a reaction independent from energetic changes must be understood as changes in $n^{\neq}$.

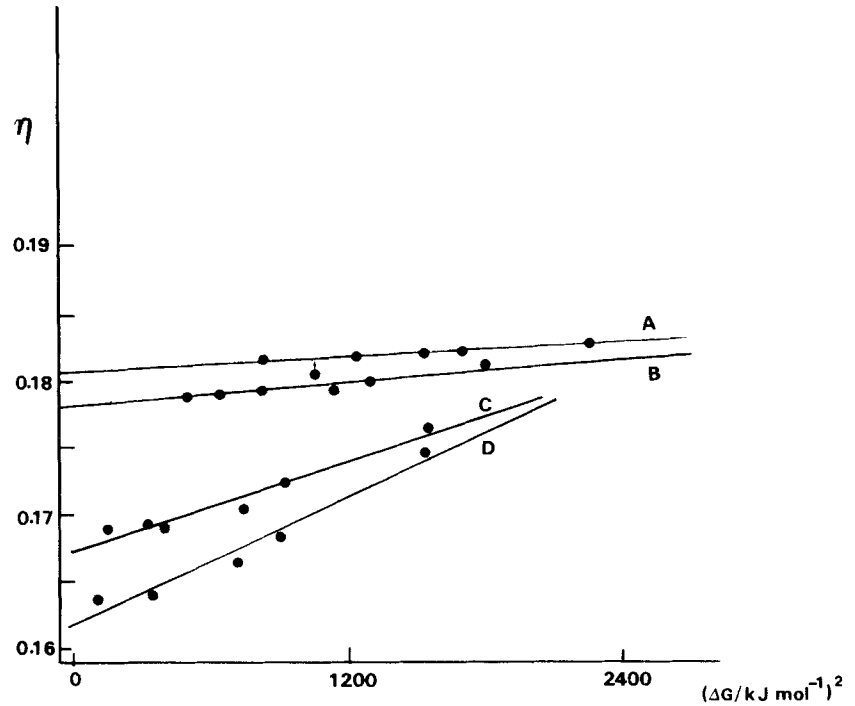

Figure 5. Solvent effects on the deprotonation of acetylacetone by carboxylate ions. (A) 100% H_2O; (B) H_2O–Me_2SO (50:50); (C) H_2O–Me_2SO (10:90); (D) H_2O–Me_2SO (5:95)

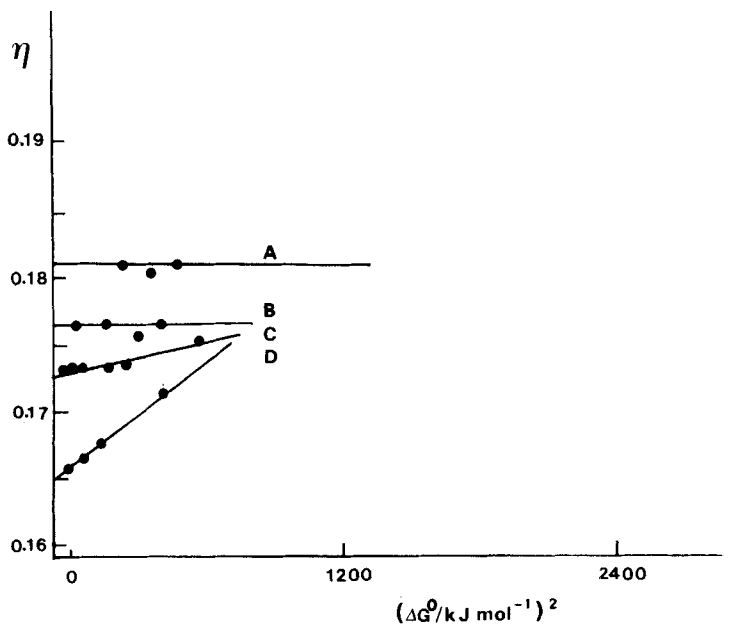

Figure 6. Solvent effects on the deprotonation of 1,3-indandione by carboxylate ions. (A) H_2O–Me_2SO (90:10); (B) H_2O–Me_2SO (50:50); (C) H_2O–Me_2SO (30:70); (D) H_2O–Me_2SO (10:90)

Figures 5 and 6 present the results of the application of ISM to the interpretation of solvent effects.

The data for acetylacetone are very clear: when we change solvent from water to water–Me_2SO(5 : 95), λ changes from 295 to 99 kJ mol^{-1}, a three-fold reduction! It is obvious that the quality of the Brønsted plot resents such a change and that is why it becomes curved.[9,23,33] The explanation that the ISM can provide for this change is also straightforward: increasing the Me_2SO content leads to poorer solvation of the carbonate ion, fewer solvent molecules will surround the transition state, which will have fewer degrees of freedom, and therefore it will be more difficult to accommodate internally the energy at the transition state and λ is lowered. It is very important to check the consistency of this result with the interpretations of λ published previously. We have shown before that the transition state's ability to accommodate internally the energy of the reaction in aqueous solutions is lower in the excited states that in the ground state of aromatic molecules.[19] This was associated with a higher rigidity of the excited states due to their increased dipole moment. For reactions in the ground state, we now demonstrate that the change to a non-hydrogen bonding solvent leads to the observation of the same effect, an increase in transition state tightness, but from a different cause, i.e. loss of molecules of the solvation shell able to accept energy of the reaction at the transition state. We can say that λ decreases with both a decrease in the number of molecules and an increase in the tightness of their association, in the transition state.

If the above reasoning is correct, we would expect Brønsted plots to be more curved for general acid–base catalysis in the excited states than in the ground states, because all the λ values calculated for excited state reactions were lower than 90 kJ mol^{-1}.[19] The recent study by Yates and McEwen[34] may substantiate this prediction. In their pioneer experimental work on acid-catalysed photohydrations of substituted styrenes and phenylacetylenes in aqueous buffer solutions, they obtained highly curved Brønsted plots. We do not interpret straightforwardly this curvature in terms of λ, because these reactions may not be adiabatic excited proton transfers and other effects may play a role.

Figures 5 and 6 also provide information about the change in $n^{\neq}$ induced by the solvent change. The relevant data are given in Table 7. In acetylacetone catalysis by carboxylate ions, the increase in $n^{\neq}$ with increase in Me_2SO content in the solvent reaches 10%. Such an increase in the transition state bond order can be understood by considering that the non-bonding electrons of the catalyst can acquire a more significant bonding character in the transition state when they are not so strongly hydrogen bonded to the solvent. This effect is significant both for the carboxylate ions and for the amines, although it is greater for the catalyst with more non-bonding electrons.

The catalysis of OH^- and H_2O shows an η value higher than expected from the other catalysis, and the discrepancy increases with increasing water content of the solution. Probably there is more than one cause for this effect. We suspect that one of the possible causes lies in the calculation of the pK_a values for these species, where it was assumed that the concentration of water on the molar scale is 55·4. Owing to the polymeric structure of water and to the hydration of OH^- and H_3O^+, the effective concentration of base to which the proton is transferred from the carbon acid may be much lower. This concentration reduction leads to an increase in the pK_a of water and a decrease in the pK_a of OH^-, both bringing the corresponding η values into better agreement with the other catalysts. However, even for a 1 M concentration there is still a significant deviation for the catalysis by OH^- and H_2O. Another factor that may

Table 7. Solvent effects, in mixtures of H_2O and Me_2SO[a]

		Proportion of H_2O (%)					
	Parameter	100	90	50	30	10	5
Acetylacetone:							
$RCOO^-$	$n^{\neq}$	0·598		0·608		0·646	0·667
	λ	295		223		117	99·4
R_2NH	$n^{\neq}$	0·600		0·605		0·633	0·650
RNH_2	$n^{\neq}$	0·584		0·586		0·608	0·624
1,3-Indandione:							
$RCOO^-$	$n^{\neq}$		0·598	0·612	0·624	0·653	
	λ		699	472	149	77·0	
R_2NH	$n^{\neq}$		0·609	0·616	0·624	0·643	
RNH_2	$n^{\neq}$		0·590	0·595	0·599	0·610	

[a]Kinetic and thermodynamic data from refs. 9 and 23. The low ratio of $(\Delta G^0/\lambda)^2$ and the limited data available for amines do not allow us to obtain good estimates of their λ values.

play an important role is the transition state bond order. It was shown that for a concerted reaction, asynchronism in the bond-making and bond-breaking processes reduces $n^{\neq}$.[22a] The origin of the asynchrony of the proton transfers to OH^- and H_2O that leads to higher η values may be related to the fact they are more strongly solvated than most other bases. This effect will operate only when the substrate itself cannot hydrogen bond to the solvent, like carbon acids, otherwise the Grotthus chain mechanism becomes possible and desolvation is not necessary.[14]

CONCLUSION

Several theoretical models of chemical reactivity take the view that several elementary reactions are not adequately described by the traditional free energy versus reaction coordinate profile[3,12,32,35,41] and two progress variables are considered, one for the mean progress and the other for the disparity progress. These kind of reactions occur when several processes (bond formation and breaking, solvation and desolvation, localization and delocalization of charge) make different progress in the transition state. The two-dimensional models have been questioned, because they bear not resemblance to potential energy surfaces current in molecular dynamics.[42] We have shown[22a] that the course of these 'imbalance reactions' can be described, as any other chemical reaction, by the traditional $\Delta G^{\neq}$ versus one-dimensional reaction energy profile through ISM.

If one wants to compare more closely ISM with these two-dimensional models, such as that of Grunwald,[41] a More O'Ferrall plot as shown in Figure 7 should be considered. It is clear from Figure 7 that the transition state bond order $n^{\neq}$ characterizes well the path of the reaction with respect to the intermediates: closer to $(\dot{A}.H.\dot{C}R_3)^-$ if $n^{\neq}$ is near 0·5 and closer to $A^-H^+CR_3^-$ if $n^{\neq}$ is near 1. Grunwald[41] defined also a disparity index in terms of the bond orders of the reactive bond orders of the intermediates, $(n_r^{\neq} - n_p^{\neq})/(n_r^{\neq} + n_p^{\neq})$. These values are not defined at $\Delta G^0 = 0$ and, in contrast

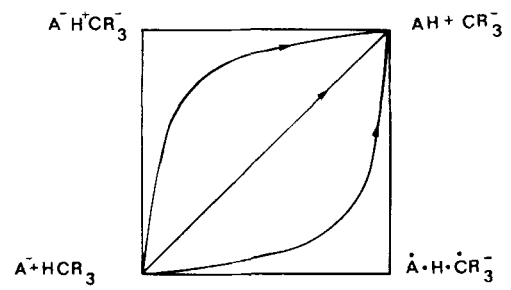

Figure 7. Two-dimensional plot for a proton transfer reaction, $A^- + HCR_3 \rightarrow AH + CR_3^-$, with intermediates of $n^{\neq} = 0{\cdot}5$ $(\dot{A}.H.\dot{C}R_3)^-$ and $n^{\neq} = 1$ $(A^-H^+CR_3^-)$

with ISM, conservation of the total bond order is always assumed, $n_r^{\neq} + n_p^{\neq} = 1$.

Within ISM the reaction progress is given by x/d ($x/d = 0$ for reactants and 1 for products) which is not independent of $n^{\neq}$. When $f_r = f_p = f$ and $\lambda \gg \Delta G^0$, then $x/d = (1/2) + (\Delta G^0/f)\ (n^{\neq}/0{\cdot}108\ l)$.[2] One might also compare the number of empirical parameters of the two models: extrinsic parameters, empirical parameters outside the field of reaction kinetics (thermodynamic and spectroscopic) and intrinsic (kinetic) parameters. ISM: extrinsic parameters f (or f_r and f_p), l and ΔG^0, and intrinsic parameters $n^{\neq}$ (for many reactions it is an extrinsic parameter) and λ; Grunwald–Marcus theory: extrinsic ΔG^0 and $\Delta G'$ (for the 'disparity reaction'), and intrinsic λ_M and μ_M (reorganization energy for the disparity reaction). Although the two models have the same number of intrinsic parameters there are, however, two important differences between them. ISM incorporates easily the asymmetry of the potential energy curves with $f_r \neq f_p$, but the Grunwald–Marcus theory is a symmetric model. Secondly, the Grunwald–Marcus theory has a quadratic dependence on ΔG^0:

$$\Delta G^{\neq} = c_0' + c_1'\ \Delta G^0 + c_2'(\Delta G^0)^2 \qquad (7)$$

whereas ISM, owing to the square dependence of $d(\eta)$ on $(\Delta G^0)^2$, controlled by λ, has the following dependence:

$$\Delta G^{\neq} = c_0 + c_1(\Delta G^0) + c_2(\Delta G^0)^2 + c_4(\Delta G^0)^4 + c_6(\Delta G^0)^6 + \cdots \qquad (8)$$

even with $f_r = f_p$; c_i and c_i' are coefficients independent of ΔG^0.

The quantitative data obtained through the intersecting state model seem to be more scattered than those treated by the Brønsted plots; this is more apparent than real, because log–log plots are insenstive to deviations. Although ISM is a sensitive model, the results obtained in this work are entirely consistent, even at a quantitative level, with those published previously. We verified that indeed $\lambda > 90\ kJ\ mol^{-1}$ for carbon acid catalysis and that $n^{\neq}$ is close to 0·55.

However, this work goes far beyond the confirmation of predicted behaviour. The application of ISM to carbon acid catalysis provides a new framework for understanding the physical meaning of the Brønsted coefficients frequently published in the literature. In fact, ISM provides a new physical meaning for β_B and α_{CH}. These coefficients are not just the result of linear free energy relationships, which tie the free energy of activation and the position of the transition state in a series of reactions to variations in the free energies of the reactions along the series. β_B is also influenced by the capacity of the transition state to accommodate internally the energy of reaction, which compensates for the conventional linear free energy effect. α_{CH} reflects a contribution from the changes in the bond orders along

a series of reactions, quantified by the electronic affinity of the carbon acids, and may show enhanced values. Accounting simultaneously for all these effects, ISM is able to provide a normalized measure of the extent of reaction.

The study of solvent effects reveals that the increase in 'intrinsic' rate constants when the solvent is changed to have a less hydrogen bonding character is due to the increase in the transition state bond order. ISM supports the existence of a curvature in Brønsted plots, but limits the observation of such reactivity–selectivity effects to the situations when λ is small and $n^{\neq}$ is small and constant.

The systematic deviation of water and hydroxide ion in Brønsted plots is rationalized essentially in terms of an increased asynchrony of the transfers of solvated protons from carbon.

ACKNOWLEDGEMENTS

This work was supported by Instituto Nacional de Investigação Científica.

REFERENCES

1. W. P. Jencks, *Chem. Rev.* **85**, 511 (1985).
2. P. E. Sørensen and W. P. Jencks, *J. Am. Chem. Soc.* **109**, 4675 (1987).
3. C. F. Bernasconi, *Pure Appl. Chem.* **54** 2335 (1982).
4. R. Ta-Shma and W. P. Jencks, *J. Am. Chem. Soc.* **108**, 8040 (1986).
5. P. Pruszynski, Y. Chiang, A. J. Kresge, N. P. Schepp and P. A. Walsh, *J. Phys. Chem.* **90**, 3760 (1986).
6. J. N. Brønsted and K. Pederson, *Z. Phys. Chem.* **108**, 185 (1924).
7. J. E. Leffler, *Science*, **117**, 340 (1953).
8. R. A. Marcus, *J. Phys. Chem.* **72**, 891 (1968).
9. C. F. Bernasconi and R. D. Bunnell, *Isr. J. Chem.* **26**, 420 (1985).
10. G. S. Hammond, *J. Am. Chem. Soc.* **77**, 334 (1955).
11. G. W. Koeppl and A. J. Kresge, *J. Chem. Soc., Chem. Commun.* 371 (1973).
12. (a) C. F. Bernasconi, *Tetrahedron* **41**, 3219 (1985); (b) C. F. Bernasconi, *Acc. Chem. Res.* **20**, 301 (1987); (c) C. F. Bernasconi, R. D. Bunnell and F. Terrier, *J. Am. Chem. Soc.* **110**, 6514 (1988).
13. F. Wiseman and N. R. Kestner, *J. Phys. Chem.* **88**, 4354 (1984).
14. A. J. Kresge, *Chem. Soc. Rev.* **2**, 475 (1973).
15. A. J. C. Varandas and S. J. Formosinho, *J. Chem. Soc., Chem. Commun.*, 163 (1986); *J. Chem. Soc., Faraday Trans. 2* **82**, 953 (1986).
16. S. J. Formosinho, *J. Chem. Soc., Perkin Trans. 2* 61 (1987).
17. S. J. Formosinho, *Rev. Port. Quím.* **27**, 427, 512 (1985).
18. S. J. Formosinho and V. M. S. Gil, *J. Chem. Soc., Perkin Trans. 2* 1655 (1987).
19. L. G. Arnaut and S. J. Formosinho, *J. Phys. Chem.* **92**, 685 (1988).
20. S. J. Formosinho and J. C. Teixeira-Dias, *J. Mol. Catal.* **42**, 127 (1987).
21. (a) S. J. Formosinho and A. J. C. Varandas, *Rev. Port. Quím.* **28**, 33 (1986); (b) S. J. Formosinho, *Rev. Port. Quím.* **28**, 38 (1986); (c) S. J. Formosinho, *Rev. Port. Quím.* **28**, 61 (1986); (d) H. D. Burrows and S. J. Formosinho, *J. Chem. Soc., Faraday Trans. 2* **82**, 1563 (1986)
22. (a) S. J. Formosinho, *Tetrahedron* **42**, 4557 (1986); (b) S. J. Formosinho, *Pure Appl. Chem.* **58**, 1173 (1986); (c) S. J. Formosinho, *J. Chem. Soc., Faraday Trans. 1*, **83**, 431 (1987)
23. S. J. Formosinho, *Tetrahedron* **43**, 1109 (1987).
24. N. Agmon and R. D. Levine, *Chem. Phys. Lett.* **52**, 197 (1977).
25. C. F. Bernasconi and P. Paschalis, *J. Am. Chem. Soc.* **108**, 2969 (1986).
26. R. P. Bell, *The Proton in Chemistry*, p. 176. Cornell University Press, Ithaca, NY (1959).
27. S. J. Formosinho, *J. Chem. Soc., Perkin Trans. 2* 839 (1988).
28. A. Pross, *Adv. Phys. Org. Chem.* **21**, 99 (1985).
29. S. S. Shaik, *J. Am. Chem. Soc.* **105**, 4359 (1983).
30. C. F. Bernasconi and S. A. Hibdon, *J. Am. Chem. Soc.* **105**, 4343 (1983).
31. N. Agmon, *Int. J. Chem. Kinet.* **13**, 333 (1981).
32. R. A. More O'Ferrall, *J. Chem. Soc. B* 274 (1970).
33. C. F. Bernasconi and F. Terrier, *J. Am. Chem. Soc.* **109**, 7115 (1987).
34. J. McEwen and K. Yates, *J. Am. Chem. Soc.* **109**, 5800 (1987).
35. D. G. Truhlar and B. C. Garrett, *Acc. Chem. Res.* **13**, 440 (1980).
36. A. J. Gordon and R. A. Ford, *The Chemist's Companion*, pp. 107 and 114. Wiley, New York (1972).
37. C. F. Bernasconi, A. Laibelman and J. L. Zitomer, *J. Am. Chem. Soc.* **107**, 6563 (1985).
38. F. Terrier, J. Lelievre, A.-P. Chartrousse and P. Farrell, *J. Chem. Soc., Perkin Trans. 2* 1479 (1985).
39. R. P. Bell and S. Grainger, *J. Chem. Soc., Perkin Trans. 2* 1367 (1976).
40. P. Kebarle and S. Chowdhury, *Chem. Rev.* **87**, 513 (1987).
41. E. Grunwald, *J. Am. Chem. Soc.* **107**, 125 (1985).
42. N. Agmon, *J. Am. Chem. Soc.* **106**, 6960 (1984).